Ocean Sci. J. (2020) 55(2):289–301
http://dx.doi.org/10.1007/s12601-020-0018-6

Article

Available online at http://link.springer.com

SpringerLink

Ocean Science Journal

pISSN 1738-5261
eISSN 2005-7172

Acoustic Characteristic of Sailfin Sandfish *(Arctoscopus japonicus)* in Dokdo, Republic of Korea

Myounghee Kang[1], Rina Fajaryanti[1], Sangchul Yoon[2], and Bokyu Hwang[3]*

[1]*Department of Maritime Police and Production System, Institute of Marine Industry, Gyeongsang National University, Tongyeong 53064, Korea*
[2]*Coastal Water Fisheries Resources Research Division, National Institute of Fisheries Science, Busan 46083, Korea*
[3]*Marine Production System Major, College of Ocean Science and Engineering, Kunsan National University, Gunsan 54150, Korea*

Received 2 September 2019; Revised 6 December 2019; Accepted 2 March 2020

Abstract – The aim of this study is to determine the acoustic characteristics of sailfin sandfish over a wide frequency range. The acoustic survey was conducted in February, May, and August 2015 off Dokdo, Republic of Korea using EK60 echosounder (18, 38, 70, 120, and 200 kHz) with the mid-water trawls. Target strength (TS) of sailfin sandfish as functions of frequency and tilt angle was modeled using the KRM (Kirchhoff-ray mode) backscatter model. The sailfin sandfish characteristics were examined by using the ΔMVBS (difference of mean volume backscattering strength) method and the net opening depth method, respectively. The acoustic signals were clearly concentrated at 20−100 m water depth. The MVBS tended to become lower as the frequency became higher. The MVBS of sailfin sandfish in the net opening depth was higher than that from the ΔMVBS method, yet both characteristics of frequency response were very similar. In comparison with the frequency response of the ΔMVBS method, that of the modeled TS was very similar in February and May. In particular, the sailfin sandfish were concentrated at 30−80 m depth and favored a temperature below 13°C. Lastly the greatest abundance of sailfin sandfish occurred in May. The highest distribution of sailfin sandfish was in the eastern part of Dokdo in February, in the west, northeastern, and southeastern areas in May, and in southeastern region in August.

Keywords – frequency response, mid-water trawl, multi-frequency, sailfin sandfish, target strength

1. Introduction

Dokdo is the easternmost island in Republic of Korea and is recognized for its historical and geographical importance. This volcanic island has unique characteristics, exhibiting all processes of geographical seamount formation. The evolution of Dokdo has involved dynamic sedimentary processes which have resulted in a variety of habitats, including gravel shores, marine plateaus, and coastal terraces (Ryu et al. 2012). The waters around Dokdo are influenced by two major currents, the North Korea cold current that moves southward from polar regions in winter and the Tsushima warm current that occurs after June. Consequently, the sea around Dokdo has a unique marine environment and is rich in nutrient sources. This means that the dynamic geological and environmental conditions generally support diverse and abundant important fishery resources (Park et al. 2002). Although Dokdo is thought to feature a rich and well-preserved biodiversity, research on marine organisms, especially fish living in Dokdo is scarce due to the difficulty accessing the island, which is 217 km from mainland Korea (Song et al. 2017). Therefore, it is essential to study and provide recent data regarding marine organisms in Dokdo. The sailfin sandfish *(Arctoscopus japonicas)* is one of the major commercial species in the Republic of Korea, and inhabits the east coast of Korea. Sailfin sandfish is a cold-water sandfish found in the east sea of Korea, the northern Sea of Japan, around the Kamchatka Peninsula, and along the Alaska coast. It is caught by diverse fisheries such as coastal gill nets, eastern sea Danish seines, eastern sea trawls, and west southern Danish seines. Its fishing ground consists mostly of areas with sand or muddy sediment, for example the continental shelf and water depths of 100−200 m (Lee et al. 2009; Yang et al. 2012). During the winter season, the sailfin sandfish migrates to the northeastern sea of Korea, where it spawns in seaweed rich areas at a depth of 2–10 m

*Corresponding author. E-mail: bkhwang@kunsan.ac.kr

(Lee et al. 2006; Yang et al. 2012). This species is managed within the total allowable catch system in force in the Republic of Korea, and this requires an accurate assessment of resources to regulate its exploitation, since the number of the species has dramatically fallen since 1970 (Yoon et al. 2018).

Regarding fisheries management using an echosounder, species identification remains a critical requirement in interpreting acoustic recordings. The rapid development of hydroacoustic systems has provided the opportunity to estimate fish abundance and biomass. This type of hydroacoustic survey has become an indispensable technique in fish stock assessment and behavioral research on fish stocks. A typical hydroacoustic survey is combined with biological sampling such as trawling, since both methods complement each other by compensating for the drawbacks of each approach. Hydroacoustic data contain extremely comprehensive information on fish densities and a general view of the overall existing fish length spectrum (Coll et al. 2007). In contrast, net sampling provides information on the fish species composition and the distribution of fish body length and weight (Elliott and Fletcher 2001). One of the goals of fisheries acoustics is to develop objective classification or identification methods to automate the allocation of acoustic backscatter to species. Relationships among frequency-dependent backscatter can be empirically derived by comparing the backscatter data to trawl catches to develop a prior criteria for classification. Traditionally, small and large targets have been separated by scrutinization and the thresholding method based on human experience, however those methods are subjective and dependent on many factors such as target size and density, and thus better methods are required. The multi-frequency method has been widely used to characterize the spectral echo signature of several species. One of the most popular techniques is the use of the difference of mean volume backscattering strength (ΔMVBS) between several frequencies. This method becomes effective in distinguishing fish species with regard to other scatters (Kang et al. 2002). The application of ΔMVBS reveals the frequency characteristics of sound scattering by marine features. The examination of the observation range is important to extract reliable information on the frequency difference of target scatters. This study employed this method to discriminate echoes generated by sailfin sandfish among other echoes and used the Kirchhoff-ray mode (KRM) backscatter model to compute the theoretical target strength (TS) to verify the ΔMVBS result. The aim of this study is to determine the acoustic characteristics of sailfin sandfish over a wide frequency range from field surveys and a theoretical TS model. It is expected that methods for determining the distribution and abundance estimates of sailfin sandfish will be enhanced.

2. Materials and Methods

Field survey

Acoustic surveys were performed around Dokdo, which lies 217 km from mainland Korea, during night time on 11−12 February, 29−30 May, and 21−22 August 2015. These surveys consisted of 8 parallel acoustic transects (Fig. 1). A total area of 407.42 km^2 with a total distance of 71.6 nm (nautical miles) was surveyed. Acoustic data were collected on RV Tamgu 20 using a scientific echosounder with five frequencies (18, 38, 70, 120, and 200 kHz, EK60, Simrad Kongsberg Maritime AS, Norway). The acoustic system was calibrated through the standard calibration method (Foote et al. 1987) before the survey on 11 November 2014. Every

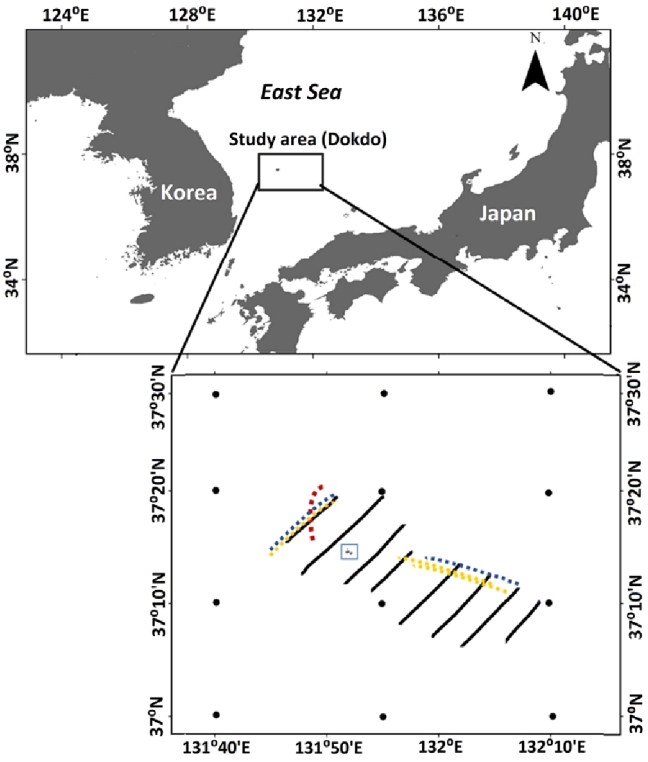

Fig. 1. The study area off Dokdo, Republic of Korea, including acoustic survey lines (black line) and mid-water trawl stations (colored dot line). The area inside the blue square is Dokdo island. Red line indicates the trawl line in February, blue line in May, and the yellow line in August. Black dot is the CTD station

Table 1. The detail specification of the echosounder

Specification	Frequency (kHz)				
	18	38	70	120	200
Power (W)	2000	2000	750	500	300
Pulse length (μs)	1024	1024	1024	1024	1024
Transducer gain (dB)	21.76	23.93	27.00	26.72	27.00
Two way beam angle (dB)	-17.0	-20.6	-21.0	-21.0	-20.7
Minor axis 3 dB beam angle (°)	10.91	6.93	7.00	6.60	6.46
Major axis 3 dB beam angle (°)	10.68	7.06	7.00	6.66	6.31
Absorption coefficient (dB/km)	2.363	9.012	22.835	40.778	59.158

frequency was simultaneously transmitted with the pulse width of 1.024 ms and ping rate of 0.24 s. A differential GPS was installed on the vessel for positioning. The detailed specifications of the sounder are presented in Table 1.

A mid-water trawl was operated to collect biological samples and verify the species composition of acoustic backscatter. This trawl was designed for fishing at relatively high speed (4−5 knots) with minimal drag. The symmetrical four-seam box had 59.3 m of head rope, 59.3 m of ground rope, and 56.1 m of side rope. One trawl was operated in February, 2 trawls were operated in May, and 4 trawls were operated in August. The net opening depth of the trawl in May and August was averaged, respectively. Details regarding trawling operations such as the locations, times and net opening depths of each trawl are shown in Table 2. The trawl was performed before acoustic acquisition or close to related acoustic data at the end of the acoustic survey. The trawl catch was separated by species and the total weight of each species was weighed. In addition, the total length and body weight of individual fish were measured.

The CTD probe (SBE19plus SeaCAT Profiler, Sea-Bird Electronics Inc, USA) was used to obtain oceanographic information. The CTD profiles were recorded at 12 stations on 6th, 7th, 11th February 2015; 29th–31st May 2015 and 1st June 2015; and 20−21st August 2015.

Data processing

Raw data of the EK60 echosounder were processed using the Echoview ver. 9 (Echoview Software Pty. Ltd, Australia). The threshold of the volume back scattering strength (S_V) was set at -78 dB, which was relatively low. The target species of the sailfin sandfish does not contain a swimbladder and weak signals including the species were considered to be included for data analysis. A function of "threshold offset" in Echoview was applied to detect noise signals by ring down and surface bubbles, and data shallower than the threshold offset were excluded from analysis. Data deeper than the seabed line were removed from the analysis. The seabed line

Table 2. The detail information of mid-water trawling such as location (start and end point), operation time, and the averaged trawl net opening mouth depth

Survey time	Location		Operation time	Mean trawl net opening depth (m)		
	Start	End		Upper depth	Center depth	Lower depth
February	37.196°N 131.498°E	37.158°N 131.495°E	2015.02.11.20:34−22:13	98.5	111.0	123.5
May	37.189°N 131.504°E	37.178°N 131.485°E	2015.05.29.20:47−21:59	83.5	96.0	108.5
	37.124°N 132.045°E	37.141°N 131.587°E	2015.05.30.19:22−20:40			
August	37.153°N 131.462°E	37.159°N 131.471°E	2015.08.21.19:04−20:20	81.1	114.8	148.6
	37.123°N 132.046°E	37.133°N 132.014°E	2015.08.22. 04:47−06:10			
	37.153°N 131.495°E	37.194°N 131.513°E	2015.08.29. 05:30−06:52			
	37.135°N 132.011°E	37.131°N 132.031°E	2015.08.29.18:08−19:22			

was selected using the maximum S_V with back step algorithm, then visually inspected and corrected. In order to increase signal-to-noise ratio (SNR), impulse noise removal and background noise removal operators were applied. The background noise removal operator estimates the background noise for each ping and subtracts it from each sample (data point). The impulse noise removal operator identifies and adjusts sample values that are significantly higher than those of surrounding samples (Echoview 2019).

The genuine frequency characteristics of the target scatters could be extracted only if the mean volume backscattering strength (MVBS) of multiple frequencies was compared at a common observation range. The observation range is determined by the SNR that is expressed as a function of target and sounder parameters, the acoustic propagation, and the noise (Kang et al. 2002). The observation range among five frequencies was found at a water depth of 150 m. Thus, acoustic data up to 150 m in all frequencies were selected and analyzed.

Two selection methods for sailfin sandfish signals

The multi-frequency technique is recognized as a reliable method to distinguish the acoustic backscatter for species classification (La et al. 2015; Kang et al. 2016). The first method to select the echo signals of sailfin sandfish was the multi-frequency technique, the so called ΔMVBS method. The ΔMVBS method depends on the frequency characteristics of sound scattering by marine features and is one of the practical identification methods that can be used over a wide range of times and waters. In accordance with the *in-situ* and *ex-situ* TS experiments of sailfin sandfish by Yoon et al. (2018), the TS difference, which can be expressed as ΔMVBS, of 38 and 120 kHz for male and female is 1 dB which is 1 dB higher at 120 kHz than at 38 kHz; however, the TS as a function of tilt angle differed approximately 3 dB between -30° and 30°. When an individual fish is swimming horizontally, the maximum TS at two frequencies, for example 38 and 120 kHz, is equal regardless of body length. However, when a fish is swimming in a certain direction, the TS directivity (i.e., TS change according to fish tilt angle) of the fish will change. The TS directivity is sharp especially at high frequency. This phenomenon occurs with regard to fish with a long body length relative to small fish (Sawada 2002; Kang et al. 2006). Thus, the tilt angles of fish, that is swimming angles, in the cell can affect the ΔMVBS. In this study, a cell size for the ΔMVBS was 5 m in the vertical and 10 pings in the horizontal, which was relatively small. The fish swimming angles in the cell could have an influence on ΔMVBS. There is no information on the natural swimming angle of sailfin sandfish. Yet, fish heading down and up of 10° would be a reasonable assumption. Accordingly, the ΔMVBS range of sailfin sandfish was set from -3 to 3 dB. The ΔMVBS was obtained from the following equation (Kang et al. 2002):

$$\Delta MVBS = MVBS\ (f_2) - MVBS\ (f_1) \quad (1)$$

where MVBS is the mean volume backscattering strength (dB), f_1 and f_2 are 38 and 120 kHz, respectively. The S_V echogram including only sailfin sandfish was extracted using the data range bitmap and mask features. The data range bitmap echogram was made in accordance with -3 to 3 dB from the S_V echogram. The mask echogram was created with the data range bitmap echogram and the S_V echogram. This procedure made echoes within the ΔMVBS range could be left and those outside the range were masked out. Finally, only sailfin sandfish echoes were displayed on the S_V echogram of 120 kHz.

The second method for determining the echo signals of sailfin sandfish is called the net opening depth method and this focuses on signals within the trawl net opening area. The echo signals were only selected between the water depth of the upper net mouth and that of lower net mouth. The net opening depth was different in every trawl. The upper, lower and center depths of the net mouth are presented in Table 2.

Theoritical model of sailfin sandfish

Acoustic scattering models provide a compatible technique to calculate the TS of a scatter which can enhance understanding on the scatter as a function of size, shape, and frequency. The TS of sailfin sandfish as functions of frequency (18, 38, 70, 120, and 200 kHz) and tilt angle (-75° to 75°) were modeled using the Kirchhoff-ray mode (KRM) backscatter model. The KRM model calculates the backscatter as a function of target length and shape, acoustic frequency, and the incidence angle. It uses the breathing mode and Kirchhoff approximations to estimate the intensity of reflected sound based on the sound speed and density contrast among water, fish body, and fish swimbladder (Clay and Horne 1994). The model results have been successfully matched to empirical measures (Horne 2003). The digital representation of the sailfin sandfish specimen was divided into 3 mm of fish body (Fig. 2). The total length of the sailfin sandfish specimen was 11.4 cm, which was the mean total length of sandfish caught in February, and the fork length was 9.9 cm. The backscatter was estimated

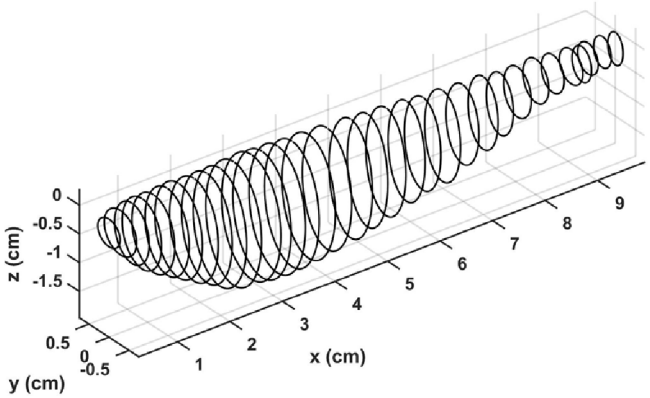

Fig. 2. The model example of a sailfin sandfish specimen (TL = 11.4 cm) reformed by digitized slicing in 3 mm. Note that the fork length was 9.9 cm

based on the size of the cylinder, the cylinder's orientation relative to the incident acoustic wave, and the acoustic carrier frequency. Backscatter from each cylinder was coherently summed to estimate the TS.

$$P_{scat}(t,R) = (P_{inc}/R)e^{i(kR-2\pi ft)}\mathcal{L}(t) \quad (2)$$

$$\sigma_{bs} = |\mathcal{L}|^2 \quad (3)$$

where k refers to the acoustic wave number (m^{-1}), f is the frequency (kHz) for the convolution of the sound wave, and $\mathcal{L}(t)$ is the scattering length (m) of the object. The scattering amplitudes generated by the fish body were added coherently to obtain the total scattering of the fish. The σ_{bs} (m^2) is the backscattering cross section of an insonified object. The TS were calculated as a non-dimensional reduced scattering length (RSL):

$$RSL = \mathcal{L}\,(L/\lambda)\,/\,L \quad (4)$$

$$TS = 20\,\log(RSL) + 20\,\log(L) \quad (5)$$

where $\mathcal{L}$ is a function of the insonifying frequency and length (L, m) of the object, λ is the acoustic wavelength (m). Little is known on the swimming angles as well as density ratio (g) and sound speed ratio (h). Thus, the g (1.04) and h (1.05) were used from Clay and Horne (1994). The acoustic characteristics at five frequencies with tilt angles (mean 0 and standard deviations of 15°, 30°, and 40°) were estimated to examine the average TS. The tilt angle of zero degree means that a fish swims horizontally without any inclination.

Frequency response

The sailfin sandfish echoes at five different frequencies were extracted in 10 m depth and 1000 m horizontally to generate graphs of the MVBS against each frequency to observe the multi-frequency characteristic. The frequency characteristic, so called frequency response, of sailfin sandfish was displayed using the MVBS by the ΔMVBS method from the water surface up to 150 m depth and the MVBS by the net opening depth method, respectively

Spatial distribution

The acoustic density in a specific layer could be expressed as the average nautical area scattering coefficient (NASC, m^2/nm^2) in the layer (Simmonds and MacLennan 2005). The distribution of sailfin sandfish was estimated using the NASC in the vertical and horizontal. For vertical distribution, the NASC was calculated for every 10 m in the vertical and entire values in the horizontal. For horizontal distribution, the NASC was determined in the entire water column data and every 1000 m in the horizontal. The vertical and horizontal

Table 3. The mid-water trawl catch in February, May, and August 2015. The number of fish, total weight by kg and percentage, total length (TL) of fish and mantle length (ML) of squid are displayed

Fish species	February 2015				May 2015				August 2015			
	Number of fish (n)	Total weight (kg)	Total weight (%)	TL and ML (cm)	Number of fish (n)	Total weight (kg)	Total weight (%)	TL and ML (cm)	Number of fish (n)	Total weight (kg)	Total weigh t (%)	TL and ML (cm)
Sailfin sandfish *(Arctoscopus japonicus)*	248	1.9	69.6	11.4	1728	39.4	76.6	15.2	792	28.9	79.8	16.8
Sparkling enope squid *(Watasenia scintillans)*	70	0.3	9.9	9.0	776	9.3	18	7.69	14	0.1	0.4	5.8
Schoolmaster gonate squid *(Berryteuthis magister)*	32	0.6	20.6	14.3	9	0.3	0.6	11.3	88	2.9	8.1	9.2
Japanese flying squid *(Todarodes pacificus)*	0	0	0	0	10	1.5	2.9	20.1	3	0.8	2.2	22.5
Hatchetfish *(Maurolicus muelleri)*	0	0	0	0	703	0.4	0.7	4.0	17	1.5	4.3	4.1
Smooth lump-sucker *(Aptocyclus ventricosus)*	0	0	0	0	1	0.5	1.0	20.8	2	1.9	5.2	28.4
Globe fish *(Takifugu porphyreus)*	1	0.7	24.5	30.4	0	0	0	0	0	0	0	0
Anchovy *(Engraulis japonicus)*	0	0	0	0	5	0.1	0.2	13.9	0	0	0	0
Total	351	3.5	100		3232	51.5	100		916	36.1	100	

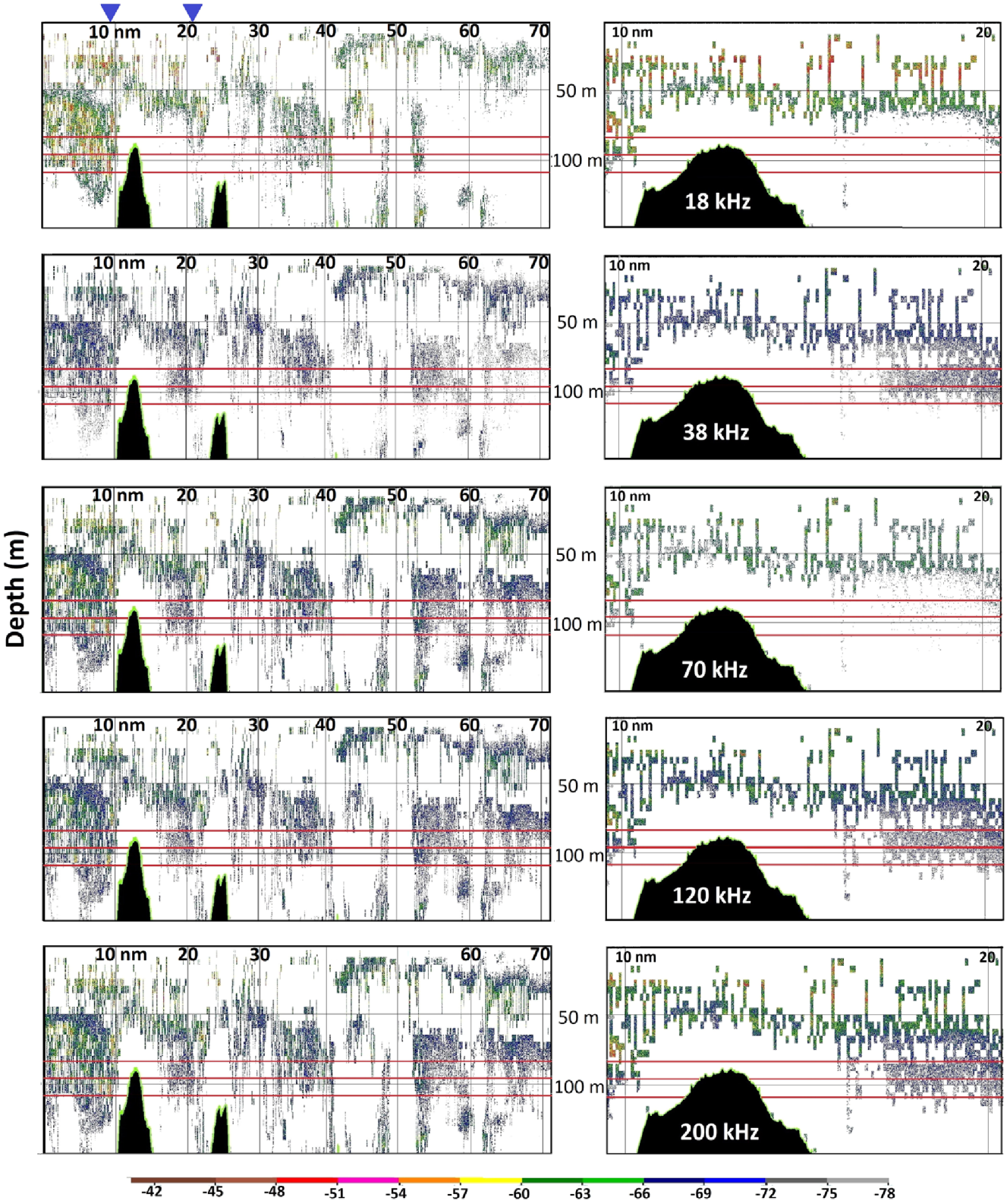

Fig. 3. The echograms display the S_V of sailfin sandfish after applying ΔMVBS method in May 2015. The five frequencies echograms over the entire survey period (left panel) and a portion of echogram (right panel) based on the blue triangle on the left panel are shown. The average depth of the upper net opening (83.5 m), that of the center net opening (96 m), that of the lower net opening (108.5 m) over entire mid-water trawls are shown in horizontal lines around 100 m water depth. The S_V color scale is inserted

distributions were expressed using the results of the ΔMVBS method and the net opening depth method, respectively.

3. Results

Catch result

On the basis of all the mid-water trawl surveys, the sailfin sandfish comprised approximately 70% of the catch by weight. The number and weight of each species caught by midwater trawl operation are shown in Table 3. The average total length of sailfin sandfish based on trawl haul was 11.4 cm in February, 15.2 cm in May, and 16.8 cm in August, respectively. Dominant species of sailfin sandfish by total weight accounted for 69.6% in February, 76.6% in May, and 79.8% in August, respectively. The largest catch was in May with the sailfin sandfish occupying 39.4 kg out of 51.5 kg in relation to the total catch weight.

The sailfin sandfish echograms

By applying the ΔMVBS method, the S_V echograms showing the backscattering strength for sailfin sandfish at 18, 38, 70, 120, and 200 kHz throughout the entire survey in May are shown in Fig. 3. It is important to compare the MVBS among multi-frequencies at a common observation range. The observation range in all frequencies was 150 m, thus the acoustic results were displayed up to 150 m. The 18 kHz S_V echogram showed the strongest backscattering strength throughout the water column which higher frequency channels were not appeared. Also, the 120 kHz frequency had relatively strong backscattering strength. The echo signals were mostly concentrated at 50–100 m depth. The distribution of echo signals was widely scattered from close to the water surface to 150 m since the survey was done at night indicating the fishes were dispersed.

Frequency response

In order to investigate the multi-frequency characteristics of sailfin sandfish, the frequency responses followed by the ΔMVBS method and the net opening depth method are compared in Fig. 4. The MVBS of sailfin sandfish based on the results of the ΔMVBS method ranged from -82.7 to -75.7 dB (February), -80.7 to -73.1 dB (May), -77.9 to -72.9 dB (August). The MVBS based on the results of the net opening depth method range from -79.3 to -70.7 dB (February), -77.6 to -67.6 dB (May), -80.0 to -74.1 dB (August). Both methods revealed that the MVBS of the sailfin sandfish showed the highest scattering levels at the lowest frequency (18 kHz),

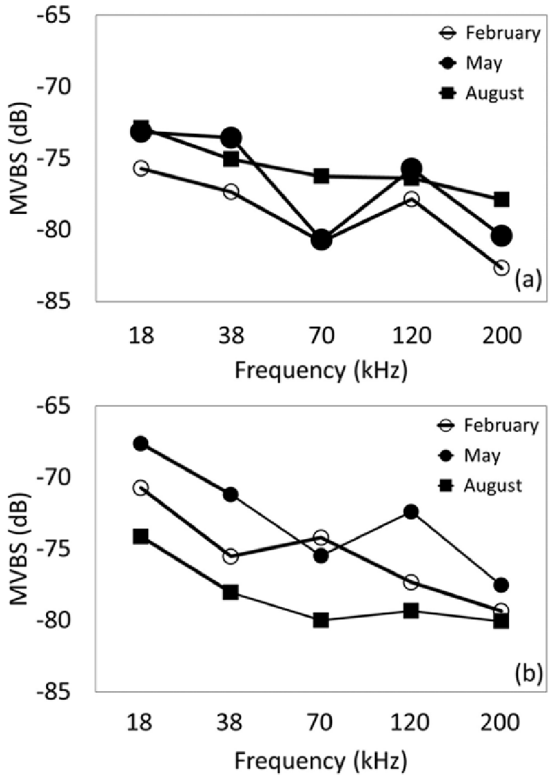

Fig. 4. The frequency response of the MVBS value from sailfin sandfish based on the applied ΔMVBS method (left) and the result of analysis inside net opening depth (right) in February, May, and August 2015

an apparent local minimum at 70 kHz, increased at 38 kHz and 120 kHz, then decreased at 200 kHz. Thus, the frequency response revealed the tendency whereby the MVBS of sailfin sandfish were smaller as the frequency was higher even though the applied ΔMVBS method showed that lowest MVBS of sailfin sandfish was found at 70 kHz in May and the net opening depth method revealed that the MVBS at 70 kHz was relatively high compared to other months.

Target strength modeled as a function of tilt angle and total length

The average TS of sailfin sandfish as a function of swimming angle (average of 0° and standard deviation of 15°, 30°, and 40°) and total length (11.4 cm, 15.2 cm, and 16.8 cm) is shown in Fig. 5. The TL stands for the average total length of sailfin sandfish caught in February, May, and August, respectively. The open circles indicate five frequencies (18, 38, 70, 120, and 200 kHz) with the standard deviation of 30°. The average TS pattern, that is TS variance, presented diverse interference patterns in the geometric scattering region.

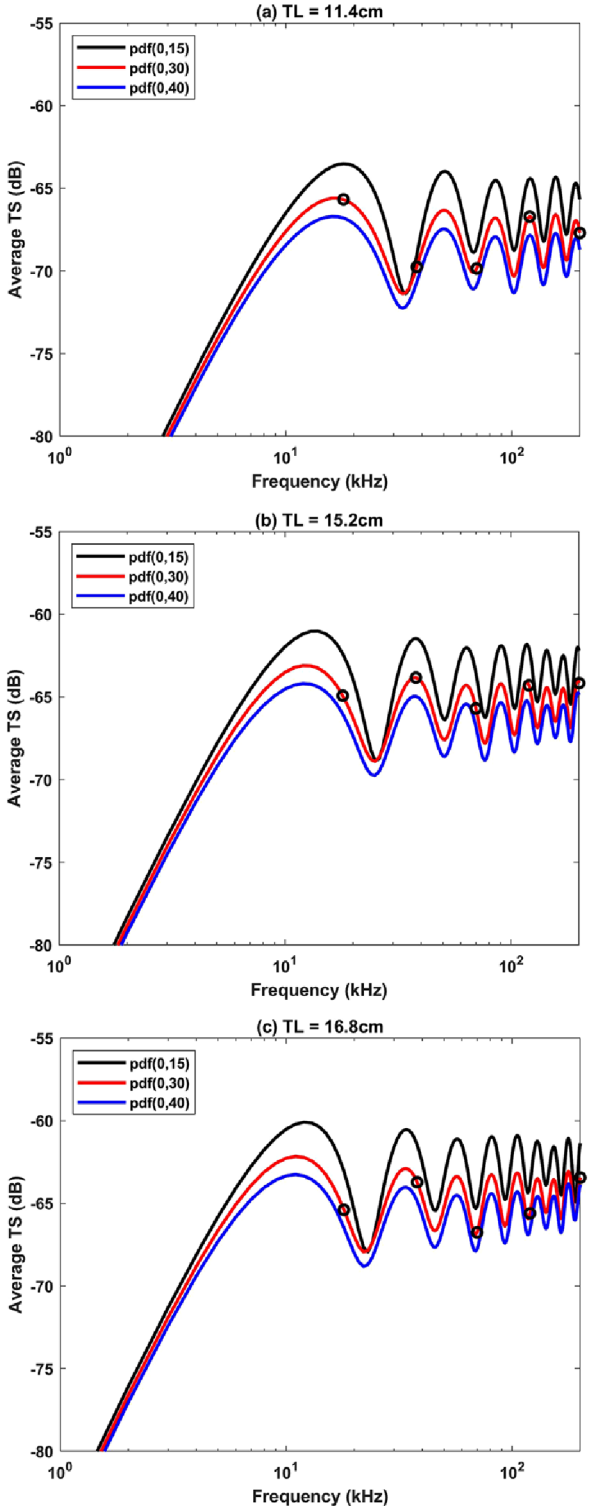

Fig. 5. The average TS on the basis of tilt angle (average of 0° and standard deviation of 15°, 30°, and 40°) for three total lengths of sandfish. The black line shows the average TS with the standard deviation of the tilt angle 15° from 1 to 200 kHz, the red and blue lines are for standard deviation of the tilt angle 30° and 40°, respectively. The open circle indicates the average TS at 18, 38, 70, 120, and 200 kHz

Namely, the variability of TS is due to the constructive and destructive interferences of pressure waves reflected within the fish body. At higher frequencies, the average TS fluctuated more often. Higher standard deviation of swimming angle at all frequencies displayed a lower average TS. The TS patterns at five frequencies for the total length of 15.2 cm and 16.8 cm were similar compared to the TS pattern for 11.4 cm. The TS difference at 38 and 120 kHz for all three lengths varied. For example, the TS difference at two frequencies for the TL of 11.4 cm with the standard deviation of 30° was approximately 3.5 dB, and that for the other two TL was relatively small. The ΔMVBS between two frequencies is equivalent to the frequency dependent TS ratio (Kang et al. 2002). According to the comparison between the frequency response of the average TS (Fig. 5) and that of MVBS applied ΔMVBS method (Fig. 4a), the TL of 11.4 cm and February, and the TL of 15.2 cm and May had similar trends although the TL of 16.8 cm and August did not correspond.

Spatial distribution of sailfin sandfish

The vertical distribution using NASC, which was attributed to sailfin sandfish, along with the vertical distribution of temperature is displayed in Fig. 6. At night time, the sailfin sandfish were distributed in dispersed layers from the surface area up to 100−150 m depth. In general, the sailfin sandfish were distributed in layers peaking at approximately 30 and 80 m depth. The NASC was higher in May than other months. In February, the highest NASC in the entire water column was 31.8 m^2/nm^2 (80 m), the lowest was 2.7 m^2/nm^2 (130 m), and an average was 12.3 m^2/nm^2. In this month, the NASC was mostly found at 30−110 m depth including the peak at 80 m. The highest NASC over the net opening was 19.1 m^2/nm^2 at the center net opening depth (110 m) and the lowest was 5.1 m^2/nm^2 around the lower net opening depth (130 m). In May, the highest NASC was 116.7 m^2/nm^2 (40 m), the lowest was 23.8 m^2/nm^2 (10 m), and an average was 57.6 m^2/nm^2. A relatively high NASC was observed across the entire water column, yet two peaks, such as at 30−40 m and 60−80 m, were found. The highest NASC over the net opening was 65.8 m^2/nm^2 around the upper net opening (90 m) and the lowest was 49.6 m^2/nm^2 around the lower net opening (110 m). The NASC in August showed the highest NASC was 40.9 m^2/nm^2 (10 m), the lowest was 3.4 m^2/nm^2 (150 m), and an average was 18.1 m^2/nm^2. The highest NASC over the net opening was 7.9 m^2/nm^2 at 130 m and the lowest was 2.8 m^2/nm^2 around the lower net opening (140 m).

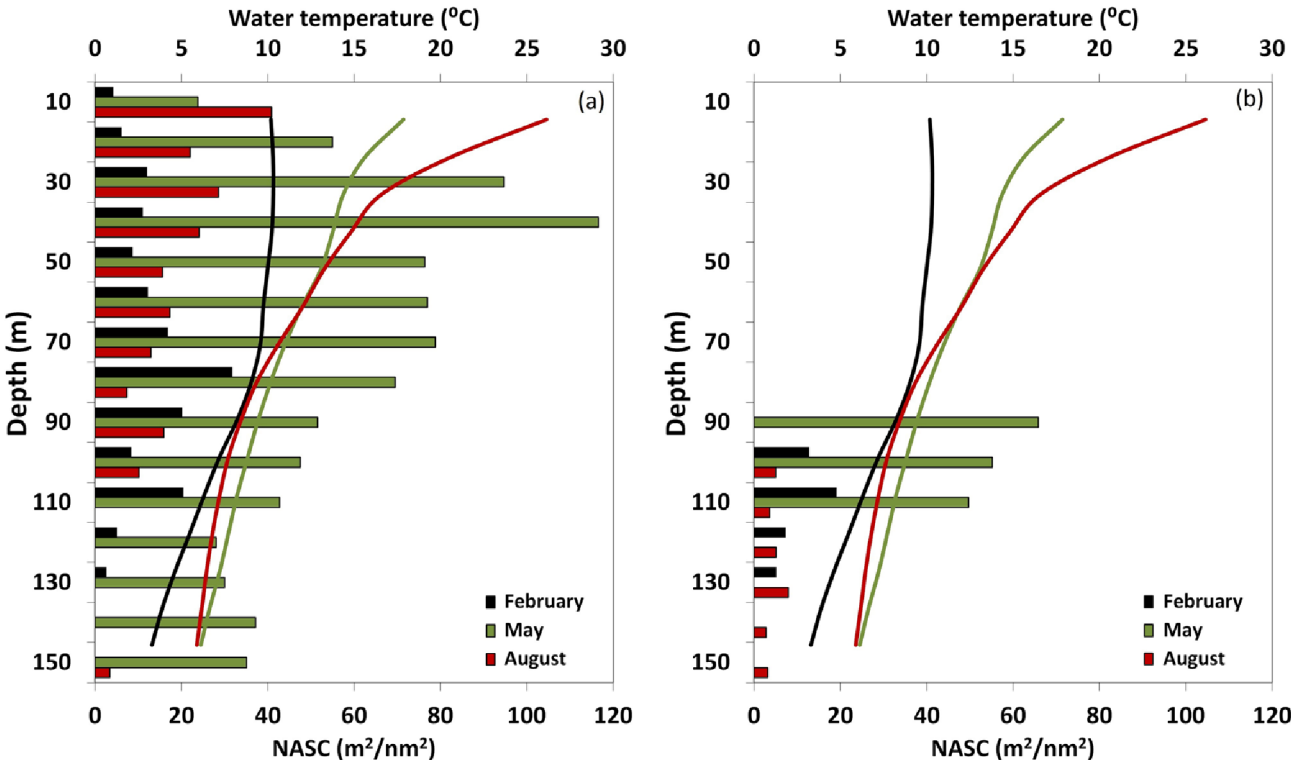

Fig. 6. The vertical distribution (NASC, m^2/nm^2) of sailfin sandfish in February, May, and August generated by ΔMVBS method (a) and at the net opening depth (b) along with the vertical profiles of water temperature (°C). The difference colors represent the different month

The temperature in the surface layer rapidly dropped from 10 m and gradually decreased. In February, the thermocline was weak, the temperature was approximately distributed from 2.8–10.4°C (mean = 6.1°C) and then gradually decreased in the 70 m depth range, which was the depth of the peak NASC from sailfin sandfish in this month. The surface temperature in May and August tended to be higher, ranging from 5.9–18.3°C (mean = 9.3°C) in May and 2.5–26.1°C (mean = 11.0°C) in August. Between water temperature and S_V from the ΔMVBS method, a positive correlation was observed only in May ($R^2 = 0.697$). The thermocline was more pronounced at the 20 m depth. The acoustic scatters were apparently concentrated in the thermocline region.

The horizontal distribution of sailfin sandfish is displayed in Fig. 7. The NASC in February was high compared to that in August, and the NASC of sailfin sandfish in May was the highest. In February, the higher NASC of sailfin sandfish occurred in the eastern part (37°8'31"N – 37°13'59"N and 131°59'49"E – 132°10'59"E) of Dokdo. In May, sailfin sandfish were highly distributed in the west toward southwestern (37°11'46" N–37°16'41"N and 131°45'43"E–131°49'55"E), northeastern part (37°15'11"N–37°17'17"N and 131°55'E–131°58'E), and southeastern part (37°8'42"N–37°13'8"N and 131°55'12"E –132°04'E) of Dokdo. In August, sailfin sandfish were mostly found in the southeastern part (37°5'42"N–37°14'35" N and 131°56'28"E–132°09'E) of Dokdo.

4. Discussion

Acoustic backscatter from narrowband echosounders used in fisheries applications (e.g. 18, 38, 70, 120, and 200 kHz) is common in the geometric scattering region where the acoustic wavelength is less than the linear dimensions of fish and macro invertebrates. In this scattering region, echo amplitude is strongly dependent on the spatial orientation of the target and its behavior (Reeder et al. 2004). The frequency characteristics of echoes not only depend on marine organisms, but also on the echosounder system, noise, and acoustic propagation. Therefore, the echograms of a multi-frequency echosounder should be carefully interpreted to derive information on the frequency characteristics of the scatters (Jech 2011). The scientific echosounder compensates for the propagation loss and displays raw S_V which compensates for sensitivities and directivities. The MVBS as the output of the echo integrator seems to be

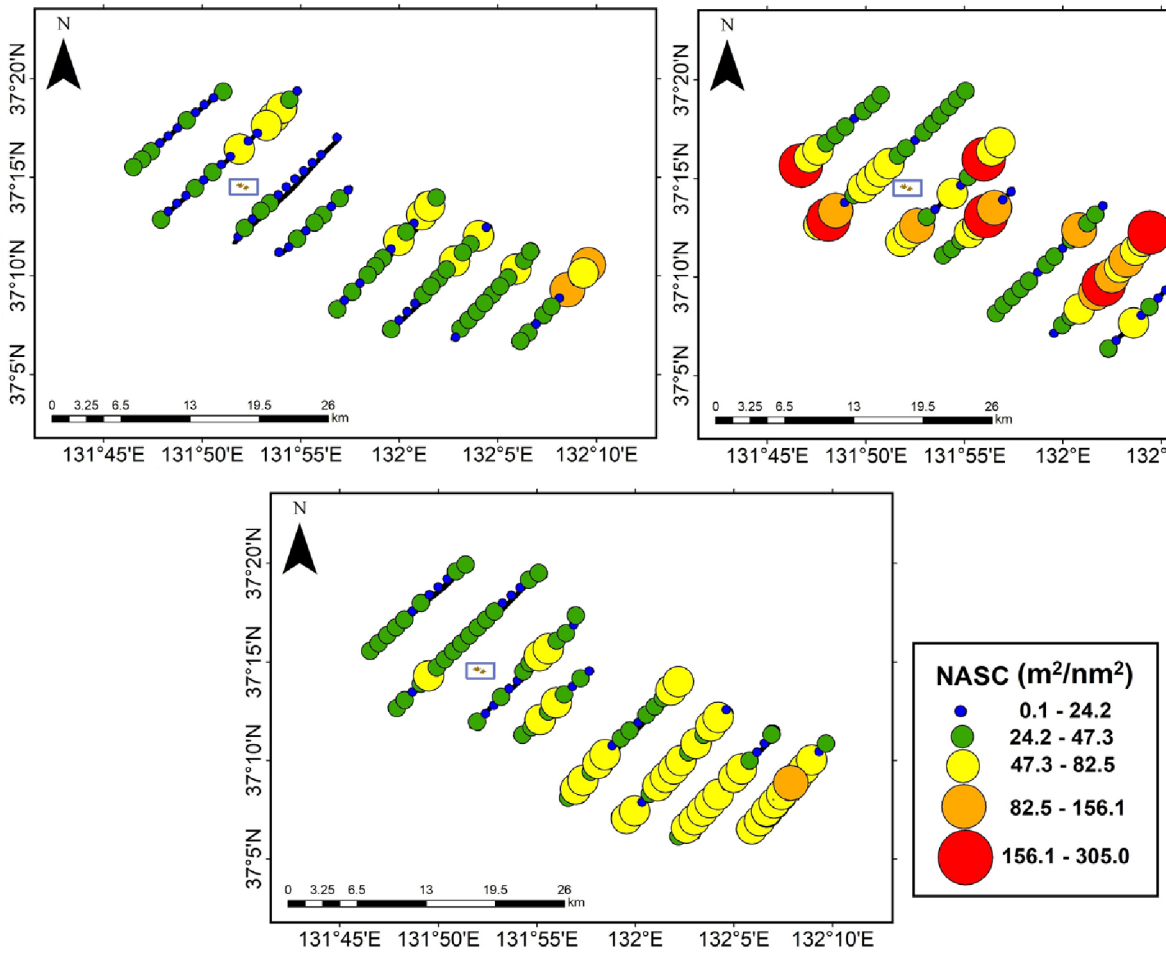

Fig. 7. The horizontal distribution of sailfin sandfish around Dokdo area (blue square). Closed circle represented the NASC of the sailfin sandfish (m^2/nm^2)

compensated for frequency-dependent factors. This is the reason for examining the frequency characteristic of scatters in a common observation range. Further, the concept of the observation range generates the ΔMVBS method more accurately (Kang et al. 2002). The choice of frequencies is potentially more important than the number of frequencies when utilizing multiple frequencies (Jech and Michaels 2006). Likewise, the volume backscatter spectra could vary widely for an individual species between aggregations. Variability in the frequency response for individual aggregations is a major challenge in relation to species discrimination (Bassett et al. 2018). The decrease of the S_V at higher frequencies is mainly due to orientation dependence, which is the sharper main lobe in the S_V pattern and the broader the orientation distribution will give a smaller S_V. The MVBS of sailfin sandfish from the net opening depth method was higher than that from ΔMVBS method, but the frequency response characteristic was similar. The frequency response of the average TS and that of MVBS applied ΔMVBS method displayed good agreement in the TL of 11.4 cm and February, and the TL of 15.2 cm and May, however, they did not agree well in the TL of 16.8 cm and August. The MVBS in a cell is attributed to species composition, sex ratio, distributions of body length and swimming angle. In this study, the sailfin sandfish comprised 70% of the trawl catch and 30% of other mixed species. One reason for the discrepancy in August could be the presence of other fish species within the sailfin sandfish aggregation or that the sailfin sandfish were segregated by size within the aggregation. Change in fish orientation and coordination could be potential to cause the change in S_V and frequency relationship. The most likely reason for the change in S_V pattern was a change in fish orientation and coordination among individuals. In an aggregating fish, this change corresponded of change in S_V pattern observed. This method of comparing multi-frequency

volume backscatter appears to be useful in detecting a change in the spatial orientation of groups of fish, such as shown for individuals (Stanton et al. 2003) and potentially for species discrimination (Lundgren and Nielsen 2008). It is well known that TS varies based on swimming angle. For sailfin sandfish, the KRM modeled TS differed around 2−8 dB by tilt angle by frequency (Fig. 5). When fish in a cell are randomly distributed, their tilt angles are averaged in the cell. Therefore, a small effect of the tilt angles of fish occurs with regard to the MVBS of the cell. But if fish in a fish school head uniformly for a certain direction in a cell, the TS will not be properly averaged across the random distribution of tilt angles. A certain tilt angle has a different influence on MVBS at various frequencies, and results in fluctuating ΔMVBS. Therefore, if there are several fish subgroups with various orientations in a fish school, a variety of ΔMVBS can be seen (Kang et al. 2006). In this study, the ΔMVBS range was set in consideration of the tilt angles of fish.

Previous studies observed a positive ΔMVBS range of squid in 38 and 120 kHz; 3.0−5.6 dB for 10.8−12.1 cm (Goss et al. 2001); 5.0 dB for the 20−23 cm mantle length (Cabreira et al. 2011); 1.3−2.5 dB for 23−27 cm (Kang et al. 2005); and 2.7 ± 3.2 dB for 24−30 cm (Peña et al. 2018). A negative $S_{V120\text{-}38}$ dB range was generated by fish and the positive $S_{V120\text{-}38}$ dB range was from squid (Cabreira et al. 2011). In this study, the range of mantle length of sparkling enope squid was 5.8−9 cm, that of schoolmaster gonate squid was 9.2−14.3 cm, and that of Japanese flying squid was 20.1−22.5 cm in the entire period of the survey. In fact, there is a possibility to include the echo signals from squids in this study. Fortunately, the mantle lengths of three squid species in this study were smaller than those in other publications. A more precise identification method for sailfin sandfish should be obtained in the near future.

The 18 kHz system potentially violated the "short-wavelength" assumption and subjected to multiple scattering effects. Wider beam widths have increased sensitivity to multiple scattering effects (Jech 2011). The 18 kHz transducer had a wider beam width than other transducers, suggesting multiple scattering effects will potentially affect the 18 kHz system more than other systems by increasing the S_V level of the 18 kHz. Beam width or pulse duration effects would not appear to be sufficiently appreciable to cause a change in the S_V relationship.

The vertical distribution of NASC from sailfin sandfish was directly related to the temperature profiles. Temperature was chosen because the water temperature was considered to be one of the key elements to affect the coastal catch level (Sakuramoto et al. 1997). The peak NASC of sailfin sandfish was associated with the thermocline or slightly below it. The low NASC during August along with the relatively low catch despite using more trawls is thought to have occurred due to the warmer temperature since sailfish sandfish could not pass when the temperature was higher than 13°C (Sakuramoto et al. 1997). Fish have similar vertical migration, they aggregate near the bottom during the daytime and ascend into middle or upper levels of water column to feed at dark when they disperse; despite the diel distribution pattern of fish, daytime acoustic surveys have underestimated fish abundance (Prchalova et al. 2003). Therefore it is recommended to carry out the acoustic survey at night when fish are found in the water column because nocturnal vertical migration brings fish into the detection range of acoustic equipment. The study area was the sandfish spawning ground from the western sea of Japan. In the spawning areas, the eggs hatch from February to March and the juveniles remain in waters with depths of approximately 10–50 m until April or May (Wanatabe et al. 2004). The sailfin sandfish were highly distributed in the eastern part of Dokdo in February. However, sailfin sandfish were found in more abundance in May at the west toward southwest, northeast, and southeastern region of Dokdo then remained abundant in the southeastern area in August. It was believed that the sailfin sandfish in the eastern population moved westwards and southwestwards for feeding purposes during spring to summer and to southeastwards for breeding purposes during autumn to winter (Yasuma et al. 2006). This species ordinarily inhabits sandy bottom areas, but in early winters it appears very close to the shore within seaweed beds for spawning. Large spawning areas are known to exist in the Akita Prefecture and the east coast of Korea. In addition, sailfin sandfish seemed to have a distinct annual migration for reproduction purposes (Ochiai and Tanaka 1986; Shirai et al. 2006).

Acknowledgements

The work was supported by the National Research Foundation of Korea (NRF) grant funded by the Korea government (MSIT) (No. NRF-2018R1A2B6005666) and supported by a grant from the National Institute of Fisheries Science (R2019023).

References

Bassett C, Roberties AD, Wilson CD (2018) Broadband echosounder measurements of the frequency response of fishes and euphausiids in the Gulf of Alaska. ICES J Mar Sci **75**(3):1131–1142. doi:10.1093/icesjms/fsx2014

Cabreira AG, Madirolas A, Brunetti NE (2011) Acoustic characterization of the Argentinean short-fin squid aggregations. Fish Res **108**:95–99. doi:10.1016/j.fishres.2010.12.003

Clay CS, Horne JK (1994) Acoustic models of fish: the Atlantic cod (*Gadus morhua*). J Acoust Soc Am **96**:1661–1668. doi:10.1121/1.410245

Coll C, de Morais LT, Lae R, Lebourges-Dhaussy A, Simier M, Guillard J, Josse E, Ecoutin JM, Albaret JJ, Raffray J, Kantoussan J (2007) Use and limits of three methods for assessing fish size spectra and fish abundance in two tropical man-made lakes. Fish Res **83**(2):306–318. doi:10.1016/j.fishres.2006.10.005

Echoview (2019) Help file 9.0.18. http://support.echoview.com/WebHelp/Echoview.htm Accessed 11 May 2019

Elliott JM, Fletcher JM (2001) A comparison of three methods for assessing the abundance of Arctic charr, *Salvelinus alpinus*, in Windermere (northwest England). Fish Res **53**(1):39–46. doi:10.1016/S0165-7836(00)00270-8

Foote K, Knudsen GHP, Vestnes G (1987) Calibration of acoustic instruments for fish density estimation: A practical guide. International Council for the Exploration of the Sea, ICES Cooperative Res Rep 69, 63 p

Goss C, Middleton D, Rodhouse P (2001) Investigations of squid stocks using acoustic survey method. Fish Res **54**:111–121. doi:10.1016/S0165-7836(01)00375-7

Horne JK (2003) The influence of ontogeny, physiology, and behavior on the target strength of walleye pollock (*Theragra chalcogramma*). ICES J Mar Sci **60**:1063–1074. doi:10.1016/S1054-3139(03)00114-0

Jech JM, Michaels WL (2006) A multifrequency method to classify and evaluate fisheries acoustics data. Can J Fish Aquat Sci **63**:2225–2235. doi:10.1139/F06-126

Jech JM (2011) Interpretation of multi-frequency acoustic data: Effects of fish orientation. J Acoust Soc Am **129**(1):54–63. doi:10.1121/1.3514382

Kang M, Furusawa M, Miyashita K (2002) Effective and accurate use of difference in mean volume backscattering strength to identify fish and plankton. ICES J Mar Sci **59**:794–804. doi:10.1006/jmsc.2002.1229

Kang DY, Tohru M, Kohji I, Hwang DJ, Jung GM (2005) The influence of tilt angle on the acoustic target strength of the Japanese common squid (*Todarodes pacificus*). ICES J Mar Sci **62**:779–789. doi:10.1016/j.icesjms.2005.02.002

Kang M, Honda S, Oshima T (2006) Age characteristics of walleye pollock school echoes. ICES J Mar Sci **63**:1465–1476. doi:10.1016/j.icesjms.2006.06.007

Kang M, Zhang H, Seo YI, Oh TY, Jo HS (2016) Exploratory study for acoustical species identification of anchovies in the South Sea of South Korea. Thalassas **32**(1):1–10. doi:10.1007/s41208-016-0013-y

La HS, Kang M, Dahms HU, Ha HK, Yang EJ, Lee H, Kim YN, Chung KH, Kang SH (2015) Characteristics of mesozooplankton sound-scattering layer in the Pacific Summer Water, Arctic Ocean. Deep-Sea Res **2**:1–10. doi:10.1016/j.dsr2.2015.01.005

Lee HW, Kim JH, Kang YJ (2006) Sexual maturation and spawning in the sandfish *Arctoscopus japonicus* in the East Sea of Korea. J Kor Fish Soc **39**(1):349–356. doi:10.5657/kfas.2006.39.4.349

Lee SI, Yang JH, Yoon SC, Chun YY, Kim JB, Cha HK, Choi YM (2009) Biomass estimation of sailfin sandfish, *Arctoscopus japonicus,* in Korean waters. Kor J Fish Aquat Sci **42**(5):487–493. doi:10.5657/kfas.2009.42.5.487

Lundgren B, Nielsen JR (2008) A method for the possible species discrimination of juvenile gadoids by broad-bandwidth backscattering spectra vs angle of incidence. ICES J Mar Sci **65**(4):581–593. doi:10.1093/icesjms/fsn031

Ochiai A, Tanaka M (1986) Ichthyology II. Koseisha-Koseikaku, Tokyo, 1139 p

Park HS, Kang RS, Myoung JG (2002) Vertical distribution of mega-invertebrates and calculation to the stock assessment of commercial species inhabiting shallow hard-bottom in Dokdo, Korea. Ocean Polar Res **24**(4):457–464. doi:10.4217/OPR.2002.24.4.457

Peña M, Roger V, Alejandro E , Alejandro A (2018) Opportunistic acoustic recordings of (potential) orangeback flying squid *Sthenoteuthis pteropus* in the Central Eastern Atlantic. J Marine Syst **179**:31–37. doi:10.1016/j.jmarsys.2017.11.003

Prchalova M, Drastik V, Kubecka J, Sricharoendham B, Schiemer F, Vijverberg J (2003) Acoustic study of fish and invertebrate behavior in a tropical reservoir. Aquat Living Resour **16**(3):325–331. doi:10.1016/S0990-7440(03)00047-0

Reeder DB, Jech JM, Stanton TK (2004) Broadband acoustic backscatter and high-resolution morphology of fish: Measurement and modeling. J Acoust Soc Am **116**:747–761. doi:10.1121/1.1648318

Ryu SH, Jang KH, Choi EH (2012) Biodiversity of marine invertebrates on rocky shores of Dokdo. Korea Zool Stud **51**:710–726

Sakuramoto K, Kitahara T, Sugiyama H (1997) Relationship between temperature and fluctuations in sandfish catch (*Arctoscopus japonicus*) in the coastal waters off Akita Prefecture. ICES J Mar Sci **54**:1–12. doi:10.1006/jmsc.1996.0164

Sawada K (2002) Study on the precise estimation of the target strength of fish. Ph.D. Thesis, Tokyo University of Fisheries, 122 p

Shirai SM, Kuranaga R, Sugiyama H, Higuchi M (2006) Population structure of the sailfin sandfish, *Arctoscopus japonicas* (Trichodontidae), in the Sea of Japan. Ichthyol Res **53**:357–368. doi:10.1007/s10228-006-0356-0

Simmonds J, MacLennan DN (2005) Fisheries acoustics: Theory and practice. Blackwell Science Ltd, Oxford, 456 p

Song SJ, Park J, Ryu J, Rho HS, Kim W, Khim JS (2017) Biodiversity hotspot for marine invertebrates around the Dokdo, East Sea, Korea: Ecological checklist revisited. Mar Pollut Bull **119**(2): 162–170. doi:10.1016/j.marpolbul.2017.03.068

Stanton TK, Reeder DB, Jech JM (2003) Inferring fish orientation from broadband-acoustic echoes. ICES J Mar Sci **60**:524–531. doi:10.1016/S1054−3139(03)00032-8

Wanatabe K, Sugiyama H, Sugishita S, Suzuki N, Sakuramoto K (2004) Estimation of distribution boundary between two Sandfish *Arctoscopus japonicas* stocks in the Sea of Japan off Honshu, Japan using density indices. Bull Jpn Soc Fish Oceanogr **68**(1):27–35

Yang JH, Lee SI, Park KY, Yoon SC, Kim JB, Chun YY, Kim SW, Lee JB (2012) Migration and distribution changes of the Sandfish, *Arctoscopus japonicus* in the East Sea. J Kor Soc Fish Tech **48**(4):401–414. doi:10.3796/KSFT.2012.48.4.401

Yasuma H, Sawada K, Miyashita K, Aoki I (2006) Swimbladder morphology and target strength of myctophid fish of the northwestern Pacific. J Acoust Soc Am **120**(5):3107–3127. doi:10.1121/1.4787575

Yoon EA, Lee K, Oh W, Choi J, Hwang K, Kang M (2018) Target-strength measurements of Sandfish *Arctoscopus japonicus*. Ocean Sci J **53**(1):73−39. doi:10.1007/s12601-017-0057-9)